Simulation of Texture Development and Induced Anisotropy of F.C.C. Polycrystals

T. Böhlke, A. Bertram
University of Magdeburg
Germany

Summary

In the present paper the deformation induced elastic anisotopy of polycrystalline copper is studied for different deformation modes using the representative volume element approach in form of the TAYLOR model.

Introduction

A tensorial and a scalar quantity describing the deviation from the isotropic elastic state is formulated for polycrystals. Furthermore an isotropy condition for discrete sets of cubic single crystals is expressed in terms of crystal orientations. Different measures describing the distance between crystal orientations are used to generate modified random orientations, which are evaluated by means of the isotropy condition. The influence of large inelastic deformations on macroscopic elastic behaviour is investigated for polycrystalline copper. The texture dependent deviation from the isotropic elastic state is estimated in terms of stiffnesses, compliances, stresses, and strains. The texture induced anisotropy is studied by an eigenvalue and eigenvector analysis of the macroscopic elasticity tensors.

Elastic Behaviour

In order to simplify the investigation and to handle the homogenization problem of polycrystalline metals in their elastic range analytically, the following assumptions are made: 1. the elastic behaviour of the aggregate is uniform; 2. the crystal orientations are constant within the grains; 3. the influence of the grain interaction, the grain boundaries, and the grain edges on the anisotropy of the macroscopic behaviour is negligible.

The stress tensor $\mathbf{T}$ in the single crystal is given as a linear map of the strain tensor $\mathbf{E}$, and vice versa. The operators of this map - the forth-order stiffness $\mathbb{\Xi}^C$ and compliance tensor $\mathbb{\Pi}^C$ - are specified by the symmetry group $\mathcal{S}$ of the material being a subgroup of the orthogonal group *Orth*

$$\mathbf{T} = \mathbb{\Xi}^C[\mathbf{E}], \qquad \mathbf{E} = \mathbb{\Pi}^C[\mathbf{T}], \qquad \mathbf{H}^T\mathbb{\Xi}^C[\mathbf{E}]\mathbf{H} = \mathbb{\Xi}^C[\mathbf{H}^T\mathbf{E}\mathbf{H}], \qquad \forall \mathbf{H} \in \mathcal{S} \subseteq \mathit{Orth}. \tag{1}$$

For hyperelastic materials the elasticity tensors possess the major symmetry. Without loss of generality, the symmetry in the first and last pair of indices is assumed. Because of the cubic symmetry there exist the following projector representations [6,7,3]

$$\mathbb{\Xi}^C = \sum_{\alpha=1}^{3} \lambda_\alpha \mathbb{\Lambda}_\alpha, \qquad \mathbb{\Pi}^C = \sum_{\alpha=1}^{3} \frac{1}{\lambda_\alpha} \mathbb{\Lambda}_\alpha, \qquad \mathbb{\Lambda}_1 = \frac{1}{3}\mathbf{I}\otimes\mathbf{I}, \quad \mathbb{\Lambda}_2 = \mathbb{\Sigma} - \mathbb{\Lambda}_1, \quad \mathbb{\Lambda}_3 = \mathbf{I}^S - \mathbb{\Sigma}. \tag{2}$$

$\mathbf{I}$ denotes the second-order identity tensor and $\mathbf{I}^S$ the symmetric part of the forth-order identity tensor. The anisotropic part $\mathbb{\Sigma}$ is given by the lattice vectors $\mathbf{g}_i$: $\mathbb{\Sigma}(\mathbf{g}_i) = \sum_{i=1}^{3} \mathbf{g}_i \otimes \mathbf{g}_i \otimes \mathbf{g}_i \otimes \mathbf{g}_i$. The projectors $\mathbb{\Lambda}_\alpha$ are idempotent $\mathbb{\Lambda}_\alpha\mathbb{\Lambda}_\alpha = \mathbb{\Lambda}_\alpha$ and biorthogonal $\mathbb{\Lambda}_\alpha\mathbb{\Lambda}_\beta = 0$ $(\alpha \neq \beta)$. The eigenvalues of the stiffness tensor are determined by its components with respect to a Cartesian coordinate system as follows: $\lambda_1 = \Xi_{1111} + 2\Xi_{1122}$, $\lambda_2 = \Xi_{1111} - \Xi_{1122}$, $\lambda_3 = 2\Xi_{1212}$.

TAYLOR's and SACHS' assumption of constant strain and stress fields, respectively, yield the most simple estimation of the elastic properties of the aggregate. The macroscopic elasticity tensors are then given as volume averages of the corresponding local fields, and imply strict upper and lower bounds for the macroscopic strain energy density [13]

$$\boldsymbol{\Xi}^V = \frac{1}{V}\int_V \boldsymbol{\Xi}^C \mathrm{d}V, \qquad \boldsymbol{\Pi}^R = \frac{1}{V}\int_V \boldsymbol{\Pi}^C \mathrm{d}V. \tag{3}$$

In general, these volume averages are anisotropic. An estimation of the properties with the additional assumption of uniformly distributed grain orientations follows by transforming the integrals (3) to the orientation space g and setting the orientation distribution function f equal to one [5]. If the orientation space is parametrized by EULER angles, one obtains with $\mathrm{d}V/V = f\mathrm{d}g = \sin(\Phi)\mathrm{d}\Phi\mathrm{d}\varphi_1\mathrm{d}\varphi_2/8\pi^2$

$$\boldsymbol{\Xi}^{VI} = \frac{1}{8\pi^2}\int_g \boldsymbol{\Xi}^C \sin(\Phi)\mathrm{d}\Phi\mathrm{d}\varphi_1\mathrm{d}\varphi_2, \qquad \boldsymbol{\Pi}^{RI} = \frac{1}{8\pi^2}\int_g \boldsymbol{\Pi}^C \sin(\Phi)\mathrm{d}\Phi\mathrm{d}\varphi_1\mathrm{d}\varphi_2. \tag{4}$$

The integration yields the well-known isotropic elasticity tensors, which imply strict bounds for the isotropic behaviour [16,15,9].

It can be shown that the isotropic bounds (4) solve the minimum problems $\| \boldsymbol{\Xi}^C - \boldsymbol{\Xi}^I \| \rightarrow \min$ and $\| \boldsymbol{\Pi}^C - \boldsymbol{\Pi}^I \| \rightarrow \min$, respectively, with $\boldsymbol{\Xi}^I$ and $\boldsymbol{\Pi}^I$ isotropic forth-order tensors and $\| \boldsymbol{\Xi} \| := (\Xi_{ijkl}\Xi_{ijkl})^{1/2}$. This result is straight-forward if the projector representation of the isotropic elastic law is used, e.g., in terms of stiffnesses

$$\| \boldsymbol{\Xi}^{C,V} - \lambda_1\boldsymbol{\Lambda}_1^I - \lambda_2\boldsymbol{\Lambda}_2^I \| \rightarrow \min \qquad \Rightarrow \qquad \lambda_1 = \frac{1}{3}\Xi_{iikk},\ \lambda_2 = \frac{1}{5}\left(\Xi_{ikki} - \frac{1}{3}\Xi_{iikk}\right). \tag{5}$$

The isotropic projectors are given by $\boldsymbol{\Lambda}_1^I = \frac{1}{3}\mathbf{I}\otimes\mathbf{I}$ and $\boldsymbol{\Lambda}_2^I = \mathbf{I}^S - \boldsymbol{\Lambda}_1^I$. The isotropic estimations by VOIGT and REUSS represent the isotropic elastic laws nearest to both the single crystal law (1) and the volume averages (3). This interpretation motivates the use of the FROBENIUS norm to formulate equivalent measures.

For aggregates consisting of a finite number of cubic single crystals with arbitrary size, the difference of the anisotropic and isotropic averages can be expressed as (V: volume of the aggregate, V^α: volume with the orientation $\mathbf{g}_i^\alpha$, $\upsilon^\alpha = V^\alpha/V$)

$$\boldsymbol{\Xi}^V - \boldsymbol{\Xi}^{VI} = \| \boldsymbol{\Xi}^C - \boldsymbol{\Xi}^{VI} \| \boldsymbol{\Delta}, \qquad \boldsymbol{\Pi}^R - \boldsymbol{\Pi}^{RI} = \| \boldsymbol{\Pi}^C - \boldsymbol{\Pi}^{RI} \| \boldsymbol{\Delta}, \tag{6}$$

with $\boldsymbol{\Delta} = (\mathbf{I}\otimes\mathbf{I} + 2\mathbf{I}^S - 5\sum_{\alpha=1}^N \upsilon^\alpha \boldsymbol{\Sigma}(\mathbf{g}_i^\alpha))/\sqrt{30}$. The distance between the averages is influenced on the one hand by the degree of anisotropy of the single crystals through, e.g., $\| \boldsymbol{\Xi}^C - \boldsymbol{\Xi}^{VI} \|$, and on the other hand by the orientation distribution in form of the tensor $\boldsymbol{\Delta}$. This representation implies the isotropy condition in terms of the N crystal orientations: $\boldsymbol{\Delta} = \mathbf{0}$. With the proper orthogonal tensor $\mathbf{Q}^\alpha = \mathbf{g}_i^\alpha \otimes \mathbf{e}_i$ one obtaines an equivalent formulation

$$\Delta_{ijkl} = 0 \qquad \Leftrightarrow \qquad \sum_{\alpha=1}^{N} \upsilon^\alpha \sum_{k=1}^{3} Q_{ik}^\alpha Q_{jk}^\alpha Q_{mk}^\alpha Q_{nk}^\alpha = \frac{1}{5}\left(\delta_{ij}\delta_{mn} + \delta_{im}\delta_{jn} + \delta_{in}\delta_{jm}\right). \tag{7}$$

The right hand side of eqn. (7) represents a special case of the general isotropic forth-order tensor. The norm $\| \boldsymbol{\Delta} \|$ is equal to one for a single orientation, equal to zero for a uniform orientation distribution, and in the interval $(0, 1)$ otherwise. $\| \boldsymbol{\Delta} \|$ can be interpreted as material independent measure for the anisotropy of the aggregate within the class of f.c.c. polycrystals.

The deviation from the isotropic elastic state of the aggregate can be expressed in terms of stiffnesses, compliances, stresses and strains. Starting from eqn. (6) and applying compatible norms for second- and forth-order tensors, one obtains the following material dependent estimations

$$\frac{\| \Xi^V - \Xi^{VI} \|}{\| \Xi^{VI} \|} = f_1 \| \Delta \|, \qquad \frac{\| \Pi^R - \Pi^{RI} \|}{\| \Pi^{RI} \|} = f_2 \| \Delta \|, \tag{8}$$

$$\frac{\| \mathbf{T}^V - \mathbf{T}^{VI} \|}{\| \mathbf{T}_F^{lower} \|} \leq f_3 \| \Delta \|, \qquad \frac{\| \mathbf{E}^R - \mathbf{E}^{RI} \|}{\| \mathbf{E}_F^{lower} \|} \leq f_4 \| \Delta \|. \tag{9}$$

As examples for both a weakly and strongly anisotropic material, the coefficients for aluminum and copper are given: $f_1^{Al} = 0.043$, $f_2^{Al} = 0.098$, $f_3^{Al} = 0.260$, $f_4^{Al} = 0.401$, $f_1^{Cu} = 0.237$, $f_2^{Cu} = 0.570$, $f_3^{Cu} = 1.740$, $f_4^{Cu} = 3.14$. For the derivation of the coefficients f_3 and f_4, the lower bound flow stress and strain ($\mathbf{T}_F^{lower}$ and $\mathbf{E}_F^{lower}$) have been estimated by the tension test.

Generation of Initially Isotropic Orientation Distributions

In order to solve the homogenization problem in form of the Taylor model, a discrete initial orientation distribution is required. In the present work, modified random distributions instead of exact solutions of eqn. (7) are used. The quality of these distributions is evaluated by means of the residuum of the isotropy condition (7). In order to calculate uniformly distributed random orientations from uniformly distributed random numbers in $\mathcal{R}^3$ one has to ensure the compatibility of the Jacobian of the transformation with the volume element of the orientation space [5]: $\mathrm{d}x_1\mathrm{d}x_2\mathrm{d}x_3 \equiv \det(\partial x_i/\partial\varphi_j)\,\mathrm{d}\varphi_1\mathrm{d}\varphi_2\mathrm{d}\varphi_3 \stackrel{!}{=} \mathrm{d}g$. In this sense the following transformation is admissible: $x_1 = \sqrt{2}\varphi_1/4\pi$, $x_2 = \sqrt{2}\varphi_2/4\pi$, $x_3 = -\cos(\varphi_3)$, $x_{1,2} \in [0, \sqrt{2}/2]$, $x_3 \in [-1, 1]$.

It can be shown that the anisotropy in terms of $\| \Delta \|$ of a set $\mathcal{M} = \{\mathbf{g}_i, i = 1 \ldots N\}$ of random orientations can be reduced, if for all pairs of different elements of $\mathcal{M}$ the distance between them is larger than a real number d_{min}, which depends on the total number of orientations. Distances have to be equal to zero for equivalent orientations and positive otherwise. An element of the symmetry group $\mathbf{H}^\alpha \in \mathcal{S}$ induces equivalent orientations [5] $\mathbf{g}_i^\alpha = \mathbf{H}^\alpha \mathbf{g}_i$ and corresponding rotations $\mathbf{Q}^\alpha = \mathbf{H}^\alpha \mathbf{Q}$. The set of all equivalent relative rotations between two crystal orientations $\mathbf{Q}_1$ and $\mathbf{Q}_2$ is given by $\mathbf{R}_{12}^\alpha = \mathbf{H}^\alpha \mathbf{R}_{12}$ with $\mathbf{R}_{12} = \mathbf{Q}_1 \mathbf{Q}_2^{-1}$. BUNGE [5] defines a distance d^B between two orientations as minimum rotation angle of all equivalent relative rotations: $d^B = \min\{\vartheta^\alpha \mid \alpha = 1..24\}$, with $2\cos(\vartheta^\alpha) = \mathrm{tr}(\mathbf{R}_{12}^\alpha) - 1$. Another distance can be defined by $d^G = \arccos(\max\{\mathbf{R}_{12} \cdot \mathbf{e}_i \odot \mathbf{e}_j \mid i, j = 1, 2, 3\})$. d^G gives the minimal length of all geodesic lines between $< 100 >$ points induced by two orientations on the unit sphere. Furthermore, the isotropy condition (7) allows the definition of a distance: $d^D = 1 - \| \Delta \|_{N=2}$. The application of the distances d^G and d^D as a filter reduces the anisotropy more than that of d^B. The mean values of $\| \Delta \|$ as a function of the number of orientations can be approximated for $d_{min} = d^G$ and $v^\alpha = 1/N$ by the following equation fulfilling the conditions $\| \Delta \|_{N=1} = 1$ and $\| \Delta \|_{N=\infty} = 0$: $\| \Delta \| \approx \exp\left(-k_1 \ln^{k_2}(N)\right)$, $k_1 = 5/4$, $k_2 = 7/10$. Fig. 1 shows the approximation of the isotropic elastic state with an increasing number of grains in terms of different variables according to eqn. (8) and (9).

Inelastic Behaviour

In this section the single crystal flow and hardening rule are introduced. The model for the single crystalline behaviour is based on the assumption that the elastic behaviour is not affected by inelastic deformations. As a result, the current elastic law is given by $\mathbf{S} = \mathbf{P}\Xi^C[\mathbf{P}^\mathrm{T}\mathbf{C}\mathbf{P} - \mathbf{I}]\mathbf{P}^\mathrm{T}$, with

$\mathbf{S} := \mathbf{F}^{-1}\mathbf{T}\mathbf{F}^{-T}$ being the material stress tensor, $\mathbf{F}$ the deformation gradient, $\mathbf{T}$ the Cauchy stress tensor, $\mathbf{C}$ the right Cauchy Green tensor, and Ξ^C the initial forth order elasticity tensor. $\mathbf{P}$ is an invertible second order tensor, called *plastic transformation* [3]. In the present work the slip system theory with the twelve (octahedral) $\{111\} < 110 >$ slip systems is applied. The plastic transformation is given by the flow rule in terms of the reference slip direction $\mathbf{d}_\alpha$, the reference slip plane normal $\mathbf{n}^\alpha$, and corresponding slip system shearing rates $\dot{\mu}_\alpha$: $\mathbf{P}^{-1}\dot{\mathbf{P}} = \sum_\alpha -\dot{\mu}_\alpha \mathbf{d}_\alpha \otimes \mathbf{n}^\alpha$. The slip rates are assumed to be governed by a power-law expression $\dot{\mu}_\alpha = \dot{\mu}_0 \text{sign}\,(\tau_\alpha)\,|\tau_\alpha/\tau_\alpha^C|^N$. The simulations are limited to proportional deformation processes. Therefore it is justified that only isotropic hardening models are taken into account. The models are specified by evolution equations for scalar strain type internal variables which determine the values of the critical resolved shear stresses. The initial values are given by $z^\alpha(t=0) = 0$. The first model is a modification of the one proposed by Peirce et al. [14,1,8]

$$\dot{z}_\beta := |\,\dot{\mu}_\beta\,|\,, \qquad \tau_\alpha^C = \tau_0^C + \sum_{\beta=1}^{12} h_S q_{\alpha\beta} z_\beta + (\tau_S - \tau_0)\tanh\left(\frac{h_0 - h_S}{\tau_S - \tau_0^C}\sum_{\beta=1}^{12} q_{\alpha\beta} z_\beta\right).$$

The modification concerns the introduction of cross-effects by $q_{\alpha\beta}$ in the last term. As a second model a power law form is used [10,4]

$$\dot{z}_\alpha = \sum_{\beta=1}^{12} q_{\alpha\beta}\frac{h_0}{\tau_S}(1 - z_\alpha)\,|\,\dot{\mu}_\beta\,|\,, \qquad \tau_\alpha^C = \tau_0^C + \tau_S z_\alpha.$$

The third model employed in this paper is given by [12]

$$\dot{z}_\beta := |\,\dot{\mu}_\beta\,|\,, \qquad \tau_\alpha^C = \tau_0^C + \sum_{\beta=1}^{12} H q_{\alpha\beta}(1 - \exp(-B z_\beta)).$$

The material under consideration is OFHC copper. The elastic constants are given by $\Xi_{1111} = 168$GPa, $\Xi_{1122} = 121$GPa, $\Xi_{1212} = 75$GPa. The reference shearing rate is taken as $\dot{\mu}_0 = 1/1000$s and the inverse strain rate sensitivity as $N = 20$. The initial critical shear stress is assumed to be equal for all slip systems and is set to $\tau_0^C = 16$MPa. The parameters of the first model are taken from [18] with exception of τ_S which is due to the above mentioned modification of the model. The parameters of the second model are identical to those used in [10,4,18]. The parameters specifying the third model are chosen such that the polycrystal stress-strain curve given by the second model is fitted. The parameters are: model 1 ($\tau_S = 100$MPa, $h_0 = 132$MPa, $h_S = 7.68$MPa), model 2 ($\tau_S = 148$MPa, $h_0 = 180$MPa, $A = 2.25$), model 3 ($H = 10$MPa, $B = 15$). The matrix elements $q_{\alpha\beta}$ are equal to 1 for $\alpha = \beta$ and coplanar systems and 1.4 otherwise.

Results

The influence of inelastic deformations on the macroscopic elastic properties is documented and discussed by different authors [17,11,5]. In this paper the deformation induced elastic anisotropy is investigated by simulating a plane strain compression, a simple shear, and a drawing test. If the Taylor model is applied, deformation inhomogeneities are excluded during the inelastic process, which must be therefore considered as a crude approximation. The representative volume element consists of 1000 crystal orientations.

Fig. 2 shows the induced elastic anisotropy in terms of equations (8) and (9) for the plane strain compression test with a thickness reduction of 90 percent. The anisotropy is still increasing in this range of deformation and reaches amounts of 8 and 16 percent for the stiffnesses and compliances, respectively.

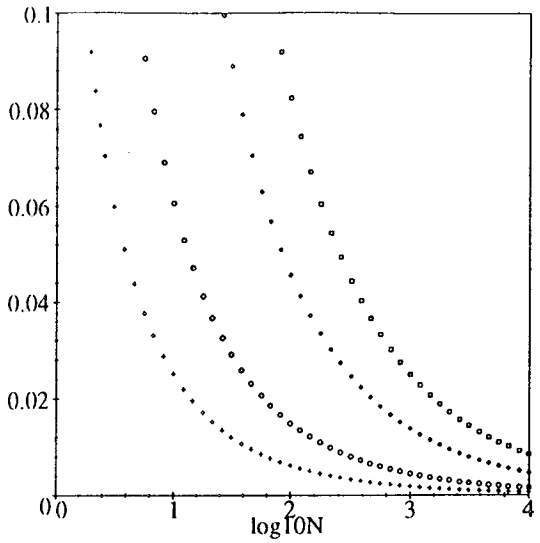

Figure 1: $f_i \| \Delta \|$ vs. $log_{10}(N)$ (+ : $i = 1$, ○ : $i = 2$, ◇ : $i = 3$, □ : $i = 4$)

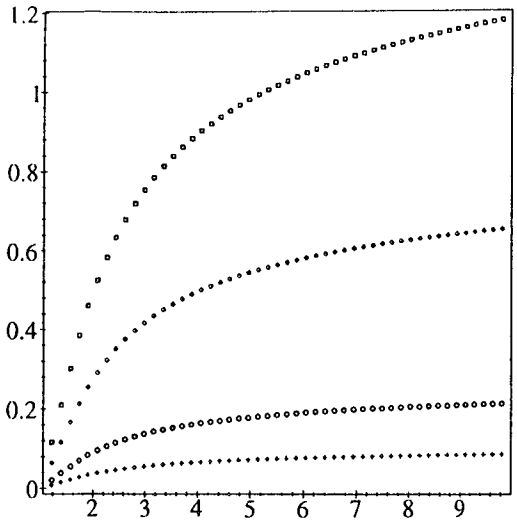

Figure 2: $f_i \| \Delta \|$ vs. F_{11} in the plane strain compression test (+ : $i = 1$, ○ : $i = 2$, ◇ : $i = 3$, □ : $i = 4$)

In fig. 3 the norm of Δ is shown for the three deformation modes versus the equivalent v.MISES strain. The induced anisotropy is much larger for the plane strain compression test than for the other two modes.

In order two investigate the influence of the employed hardening models, the predictions of the three models are compared in the simple shear test up to a shear number of $K = 10$ (fig. 4). The differences are negligible for $K < 3$. For larger shear numbers a saturation or even a slight decreasing of the anisotropy is observed.

One is confronted with the problem that the numerical values of the elasticity tensors are known relative to an arbitrary coordinate system and one wants to determine the type of anisotropy. The procedure proposed by COWIN [7] is applied to solve this problem. For the considered deformation modes the eigenvectors of Ξ^V_{ijkk} and Ξ^V_{ikkj} are all coincident and the eigenvalues of Ξ^V_{ikkj} are distinct. Therefore the material is of orthotropic symmetry. The eigenvalues of Ξ^V_{ijkk} are not affected by the inelastic deformation and are all equal to the one associated with the dilatational eigenvalue of the cubic behaviour.

References

1. Asaro, R. J. and Needleman (1985), Acta metall., Vol. 33, pp. 923.

2. Bertram, A. and Kraska, K. (1995), "Description of finite plastic deformations in single crystals by material isomorphisms", in D. F. Parker, A. H. E., editor, Proceedings of IUTAM Symposium on Anisotropy, Inhomogeneity and Nonlinearity in Solid Mechanics, pp. 77–90.

3. Bertram, A. and Olschewski, J. (1991), "Formulation of anisotropic linear viscoelastic constitutive laws by a projection method", in Freed, A. and Walker, K., editors, High temperature constitutive modelling: Theory and Application, MD-Vol. 26, AMD-Vol. 121, pp. 129–137.

4. Bronkhorst, C., Kalidindi, S., and Anand, L. (1992), "Polycrystalline plasticity and the evolution of crystallographic texture in f.c.c. metals", R. Soc. Lond. A., Vol. 341, pp. 443–477.

5. Bunge, H. (1993), Texture Analysis in Material Science, Cuviller Verlag Göttingen.

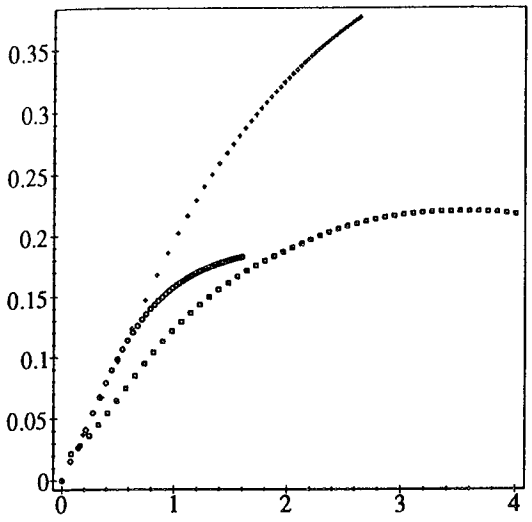

Figure 3: $\| \Delta \|$ vs. equiv. v.MISES-strain for the three deformation modes (+: plane strain compression, o: simple shear, □: drawing)

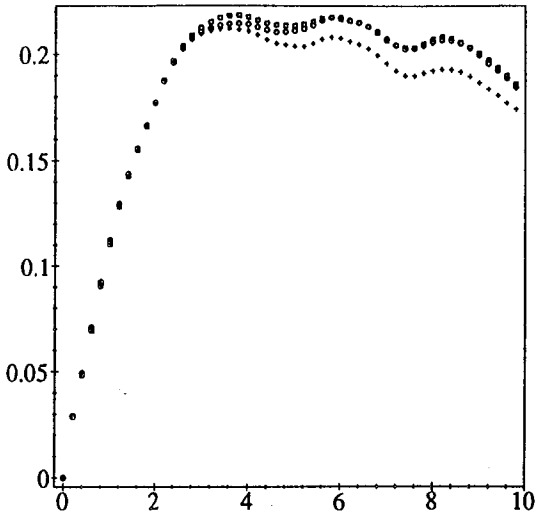

Figure 4: $\| \Delta \|$ vs. K in simple shear deformation for model 1 to 3, (+: model 1, o: model 2, □: model 3)

6. Cowin, S. (1990), "Eigentensors of linear anisotrtopic elastic materials", Q. J. Mech. appl. Math., Vol. 43, pp. 15–41.

7. Cowin, S. and Mehrabadi, M. (1987), "On the identification of material symmetry for anisotropic elastic materials", Q. J. Mech. appl. Math., Vol. 40, 451–476.

8. Harren, S., Lowe, T., Asaro, R., and Needleman, A. (1989). "Analysis of large-strain shear in rate-dependent face-centred cubic polycrystals: Correlation of micro- and macro-mechanics", Phil. Trans. R. Soc. Lond. A, Vol. 328, pp. 443–500.

9. Hill, R. (1952), "The elastic behaviour of a crystalline aggregate", Proc. Phys. Soc. Lond., A 65, pp. 349–354.

10. Kalidindi, S., Bronkhorst, C., and Anand, L. (1992), "Crystallographic texture evolution in bulk deformation processing of fcc metals", J. Mech. Phys. Solids, Vol. 40, pp. 537–569.

11. Liu, Y. and Alers, G. (1966), "The anisotropy of young's modulus in cold rolled sheets of binary Cu-Zn alloys", Trans AIME, Vol. 236, pp. 489–495.

12. Méric, L., Cailletaud, G., and Gaspérini, M. (1994), "Calculations of copper bicrystal specimens submitted to tension–compression tests", Acta metall. mater., Vol. 42, pp. 921–935.

13. Nemat-Nasser, S. and Hori, M. (1993), Micromechanics: Overall Properties of Heterogeneous Materials, North-Holland series in applied mathematics and mechanics, Elsevier Science Publishers B.V.

14. Peirce, D., Asaro, R., and Needleman, A. (1983), Acta Metall., Vol 31, pp. 1951.

15. Reuss, A. (1929), "Berechnung der Fließgrenze von Mischkristallen auf Grund der Plastizitätsbedingung für Einkristalle", Z. Angew. Math. Mech., Vol. 9, pp. 49–58.

16. Voigt, W. (1889), "Über die Beziehung zwischen den beiden Elastizitätskonstanten isotroper Körper", Wied. Ann., Vol. 38:573–587.

17. Wasserman, G. and Grewen, J. (1962), Texturen metallischer Werkstoffe, Springer.

18. Wu, P., Neale, K., and Van der Giessen, E. (1996), "Simulation of the behaviour of fcc polycrystals during reversed torsion", Int. J. Plast., Vol. 12, pp. 199–1219.

MODELING AND SIMULATION BASED ENGINEERING

Volume II

Editors: S. N. Atluri
P. E. O'Donoghue

Published by Tech Science Press

S. N. Atluri
Center for Aerospace Research and Education
University of California at Los Angeles
Los Angeles, California, U.S.A.

P. E. O'Donoghue
Department of Civil Engineering
National University of Ireland,
Galway, Ireland

Published by Tech Science Press
426 Mesa Verde Ave
Palmdale, CA 93551
e-mail: techscience@earthlink.net

Printed in the United States of America

ISBN 09657001-2-7